Rothenburg, L. & Bathurst, R. J. (1989). *Géotechnique* **39**, No. 4, 601–614

Analytical study of induced anisotropy in idealized granular materials

L. ROTHENBURG* and R. J. BATHURST†

Development of induced anisotropy during shear deformation of plane granular assemblies is investigated by introducing statistical characteristics of fabric and contact forces. The introduced microstructural parameters are explicitly related to the measure of deviatoric load by considering conditions of static equilibrium. Verification of the relationship between parameters of anisotropy, average forces and external loads is presented based on numerical simulation of tests on plane granular assemblies. The physical significance of introduced parameters of microstructure and their evolution during shear deformations is discussed.

KEYWORDS: fabric/structure of soils; granular materials; shear strength; statistical analysis; stress analysis.

Le développment de l'anisotropie induite pendant la déformation de cisaillement d'assemblages plans granulaires est examiné grâce à l'introduction de caractéristiques statistiques de la fabrique et des efforts de contact. Les paramètres microstructuraux introduits sont reliés de façon explicite à la mesure du chargement déviatorique en considérant les conditions de l'équilibre statique. La vérification de la relation entre les paramètres d'anisotropie, les forces moyennes et les chargements externes est présentée sur la base de la simulation numérique d'essais sur des assemblages plans granulaires. On analyse l'importance physique des paramètres microstructuraux introduits et leur évolution pendant les déformations de cisaillement.

NOTATION

- a second-order coefficient of contact normal anisotropy
- a_n second-order coefficient of average normal force anisotropy
- a_t second-order coefficient of average tangential force anisotropy
- $\bar{d}_0$ average particle diameter
- $E(\theta)$, $E(\mathbf{n})$ contact normal distribution function
- $\boldsymbol{f}^c, \boldsymbol{f}_n^c, \boldsymbol{f}_t^c$ contact force vector, normal and tangential (shear) contact force vector components
- $\bar{f}_n(\theta), \bar{f}_t(\theta)$ distribution of average normal and tangential (shear) contact forces
- $\bar{f}_0$ average normal contact force over all contacts
- $\boldsymbol{l}^c$, l^c contact vector, contact vector length = distance between centres of particles in mutual contact
- $\bar{l}_0$ assembly average contact vector length
- $L(l^c)$ distribution of contact vector lengths
- m_v contact density ($m_v = M/V$)
- $\Delta M(\theta_g)$ number of contact falling within group orientational interval θ_g
- M total number of assembly contacts
- $\boldsymbol{n}$ unit vector
- $\boldsymbol{n}^c$ contact normal vector
- N total number of assembly particles
- $\boldsymbol{t}^c$ contact tangent vector
- $S(\boldsymbol{l})$ joint contact vector length-orientation distribution
- V assembly area (or volume)
- ε, ε_t strain tensor, deviatoric strain $\varepsilon_t = \sqrt{((\varepsilon_{11} - \varepsilon_{22})^2 + (\varepsilon_{12} + \varepsilon_{21})^2)}$
- γ co-ordination number ($\gamma = M/N$)
- θ_a second-order principal direction of contact anisotropy
- θ_f second-order principal direction of average normal contact force anisotropy
- θ_t second-order principal direction of average tangential contact force anisotropy
- σ, σ_{ij} stress tensor
- σ_n normal invariant stress quantity
- σ_t deviatoric invariant stress quantity

INTRODUCTION

Engineering behaviour of granular materials is commonly expressed in terms of macroscopic characteristics that are ultimately based on continuum parameters like stress and strain. Much of

Discussion on this Paper closes 2 April 1990; for further details see p. ii.

* University of Waterloo, Ontario.
† Royal Military College of Canada, Kingston, Ontario.

the current research effort is directed at establishing stress–strain relationships with the ultimate objective of solving boundary value problems of engineering interest. Although a constitutive model can be developed based on a combination of experimental data and formal principles of continuum mechanics, such developments cannot guarantee that the physics of material behaviour is adequately represented in the model. Perhaps more importantly, such approaches seldom offer physical insight into the observed macroscopic behaviour of granular materials.

Another approach to constitutive modelling that offers physical understanding is to treat a granular material as an assembly of particles interacting by means of contact forces and attempt to derive stress–strain relationships on this basis. This Paper is a contribution toward that goal and it considers in detail a relationship between the stress tensor and averages of microscopic parameters, contact orientations and contact forces. The emphasis of the Paper is on the physical aspects of the relationship between stresses, average contact forces and characteristics of a generally anisotropic fabric of granular materials. A direct link between the measure of deviatoric load and a parameter of fabric anisotropy presented in the Paper emphasizes the well-known phenomenon of induced anisotropy in sands.

Most analytical developments in the Paper are limited to relationships between micro- and macro-parameters for a two-dimensional analog of granular materials represented by plane assemblies of discs. The introduction of this model system dates back to the work of Schneebeli (1956) on assemblies of metal rods. Experimental work with assemblies of discs made of optically sensitive materials (e.g. Dantu, 1957, 1968; Oda, 1972a, b, c; de Josselin de Jong & Verruijt, 1969; Drescher & de Josselin de Jong, 1972; Oda & Konishi 1974a, b) have provided qualitative understanding of mechanisms of load transfer in granular materials. More recent work using numerical simulation of plane assemblies of discs (e.g. Cundall & Strack 1979a, b; Cundall, Drescher & Strack, 1982; Thornton & Barnes, 1986; Bathurst & Rothenburg, 1988a, b) offers a unique opportunity to obtain complete quantitative information on all microscopic features of an assembly of particles. These studies can guide theoretical developments that are based on a micromechanical approach to stress–strain behaviour of granular media.

The search for explicit relationships between stress tensor and parameters that describe interparticle forces and fabric has been the subject of a number of papers beginning with the work by Dantu (1957) and Weber (1966). Since then the problem has been pursued by others such as Mehrabadi, Nemat-Nasser & Oda (1982), Cundall & Strack (1983) and Thornton & Barnes (1986). A common starting point in these previous investigations is a relationship between the average stress tensor and intergranular forces. Thereafter, the differences are in the statistical treatment of microscopic information, averaging techniques and the ease with which the final result can be physically interpreted. The approach used in the current investigation resembles one that could be adopted by an experimenter who has complete information on all microscopic features of a granular assembly and attempts to establish regular trends from an overwhelming volume of seemingly random data. In the current study a few simple parameters are introduced that describe average characteristics of contact forces and fabric. These parameters are then explicitly related to mobilized friction angle in granular materials.

The established relationships are verified using numerical simulation of a biaxial compression test on an assembly of discs comprising 1000 particles. In addition, the results of this numerical simulation have been used to trace the evolution of internal forces and characteristics of stress-induced fabric anisotropy and to illustrate the physical significance of parameters involved.

QUALITATIVE FEATURES OF LOAD TRANSFER IN GRANULAR ASSEMBLIES

Important qualitative features of load transfer in granular assemblies can be conveniently illustrated by reference to an experiment on an assembly of photo-elastic discs. The pattern of line segments reproduced in Fig. 1(a) after de Josselin de Jong & Verruijt (1969) represents orientations and magnitudes of interparticle forces in an assembly of discs confined within rectangular platens. The assembly is under deviatoric boundary load. The thickness of lines is proportional to the magnitude of contact forces. Higher forces can be identified with contacts oriented towards the direction of maximum boundary load. To emphasize this bias, Fig. 1(b) and (c) illustrate groups of vertical and horizontal load-bearing contacts represented by lines connecting centres of particles. The difference between the numbers of vertical and horizontal contacts is a measure of geometrical anisotropy in microstructure of the assembly. The fact that vertical and horizontal contacts also carry forces of distinctly different magnitudes illustrates an important link between microscopic geometry and characteristics of load transfer. Although forces acting at contacts with similar orientations vary in a seemingly random

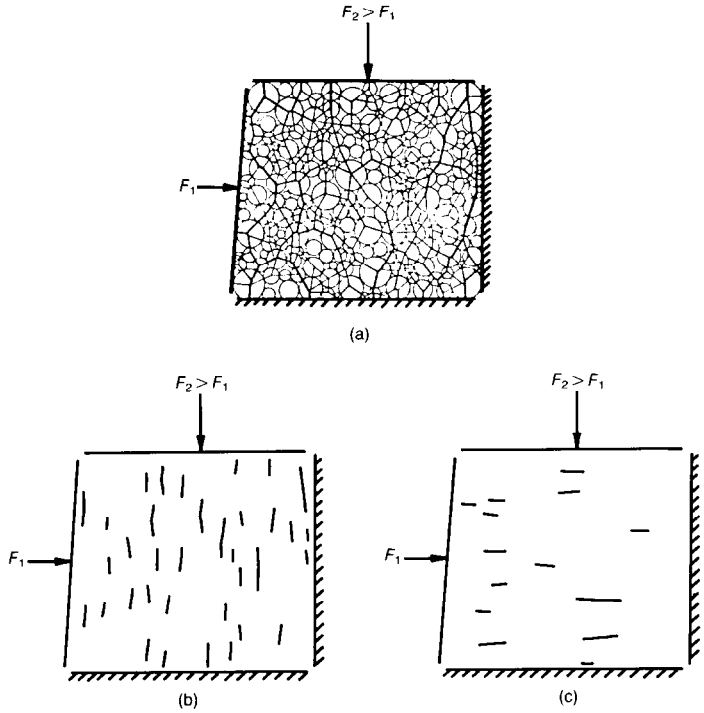

Fig. 1. Biaxial compression test on an assembly of photo-elastic discs (after de Josselin de Jong and Verruijt, 1969): (a) distribution of contact forces; (b) vertical contacts; (c) horizontal contacts

manner, average forces over such groups are constrained by conditions of static equilibrium and characteristics of fabric. As such, parameters describing average forces and anisotropy in contact orientations can be related to boundary loads. The primary objective of this Paper is to establish this relationship.

MICROSCOPIC CHARACTERISTICS OF GRANULAR ASSEMBLIES

During shearing deformations, cohesionless granular assemblies exhibit continuous changes in the evolution of interparticle forces and internal geometry. In particular, shearing deformations lead to changes in magnitude and distribution of interparticle forces. Simultaneously, there are changes in the number of load-carrying contacts and their distribution of orientations. Basic concepts related to mechanisms of load transfer can be introduced empirically by referring to a numerically simulated biaxial test carried out on the assembly of 1000 discs shown in Fig. 2(a) and reported by Bathurst (1985). The stress–strain curves for this test are shown in Fig. 2(b). The geometry and contact forces in the simulated assembly under initial hydrostatic conditions and at peak stress ratio are illustrated in Figs. 3(a) and 4(a).

CHARACTERISTICS OF FABRIC

Contact density

An instantaneous geometrical state of an assembly of N particles can be characterized by the average co-ordination number of the assembly $\gamma = M/N$, where M is twice the number of physical contacts. A similar characteristic which is a convenient descriptor in later developments is the assembly contact density m_v where

$$m_v = M/V \tag{1}$$

Here V is the volume of the assembly (or its area in the plane case). Fig. 2(c) illustrates reduction in co-ordination number (or contact density) during shearing deformations and is consistent with macroscopically observed dilation.

Contact density is a limited descriptor of the state of packing as it carries no information on orientations of interparticle contacts. Considering that intergranular forces are strongly dependent on orientation of contacts (Fig. 1), complete description of load transfer in granular assemblies

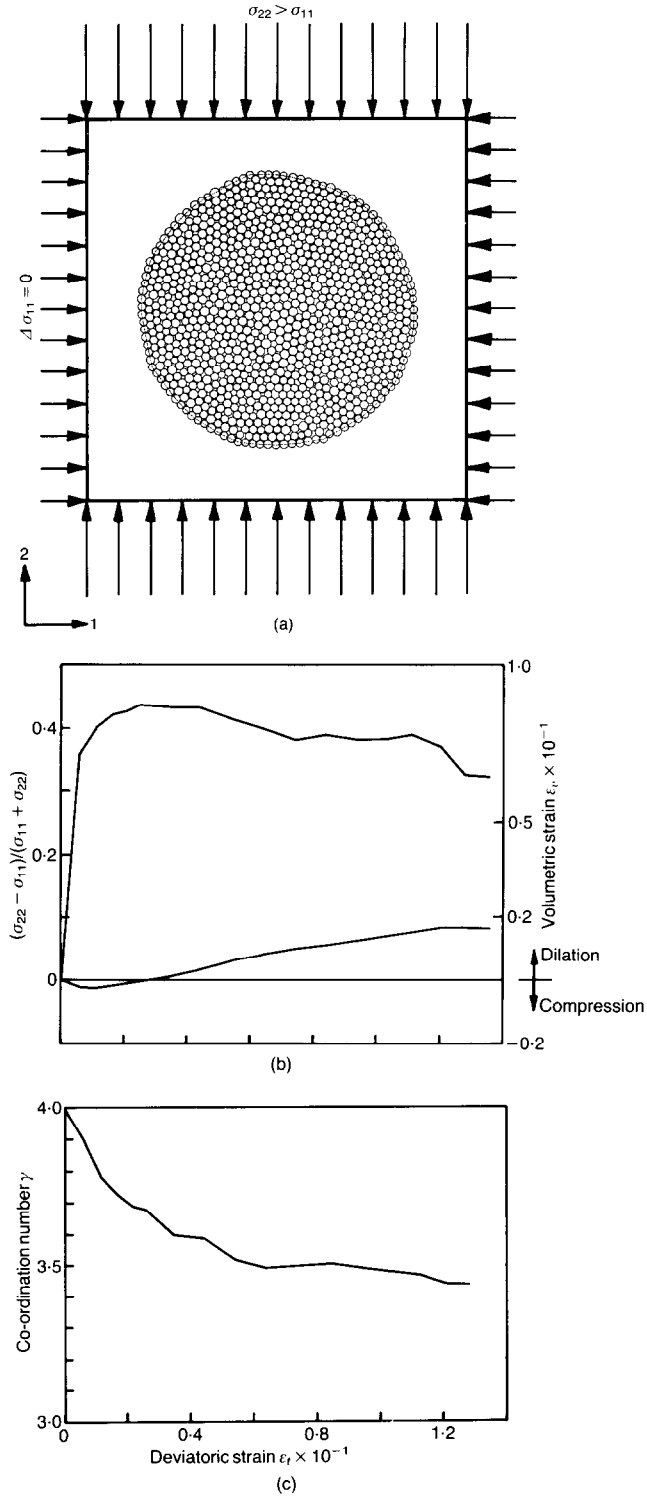

Fig. 2. Results of numerically simulated biaxial compression test: (a) biaxial compression test on 1000 disc assembly; (b) stress–strain response; (c) co-ordination number against deviatoric strain

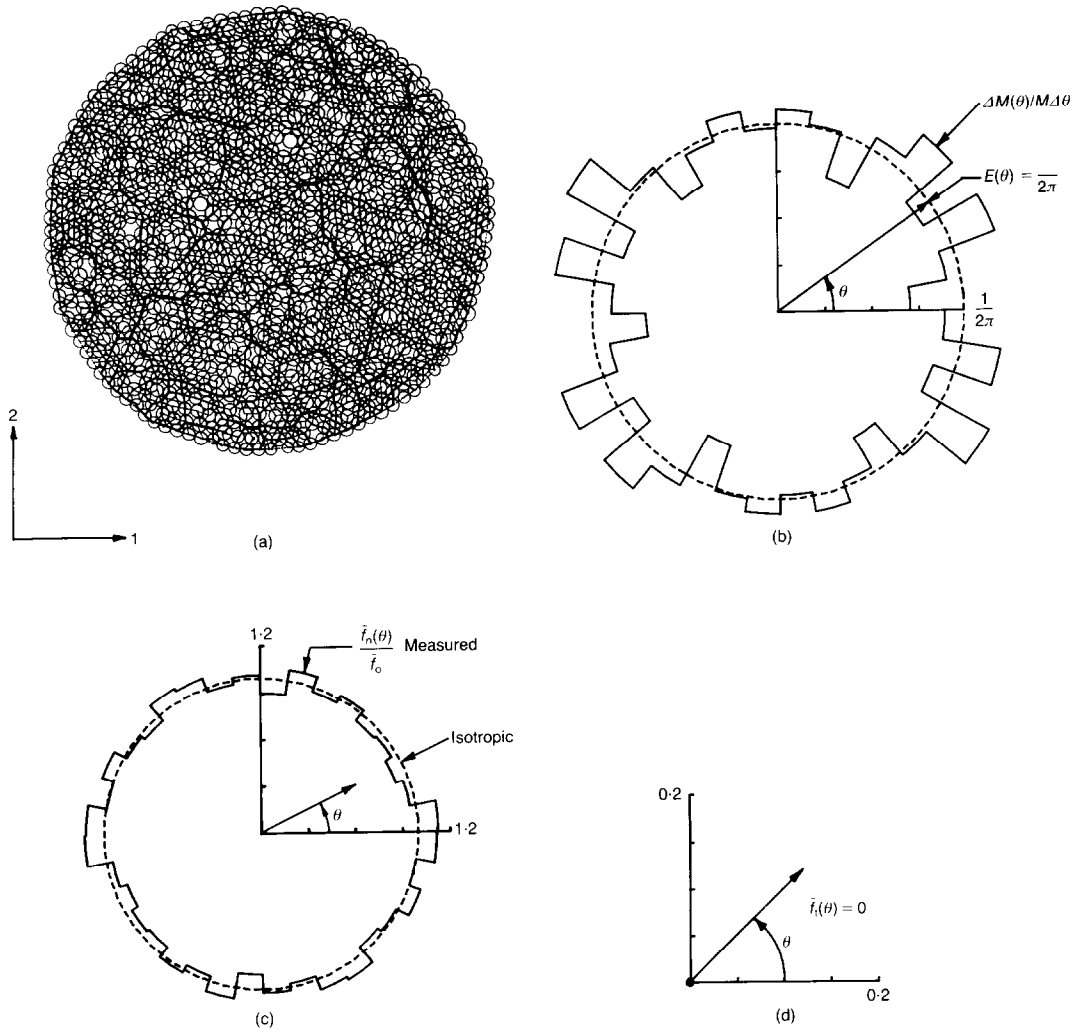

Fig. 3. Distribution of contact normals and average interparticle force components: (a) assembly at initial (hydrostatic) stress condition; (b) initial distribution of contact normals; (c) initial distribution of average normal forces; (d) initial distribution of average tangential forces

requires information on the distribution of contact orientations.

Contact orientations

Orientations of contacts for plane assemblies of discs can be characterized by an angular distribution $E(\theta)$ defining the portion of contacts $\Delta M(\theta)$ falling within an angular interval $\Delta\theta$. The polar histogram in Fig. 3(b) characterizes contact orientations for the initial state of the test in Fig. 3(a) when the assembly contains about 2000 physical contacts. The assembly can be considered geometrically isotropic in the sense that there is no systematic bias in the number of contacts of any particular orientation. To illustrate this point further, the circular distribution in Fig. 3(b) is visually adequate to approximate the empirical histogram.

During shear deformations, contacts oriented along the direction of maximum tensile strain disintegrate more rapidly than contacts of other directions. Consequently, the distribution of contact orientations becomes markedly anisotropic, as illustrated in Fig. 4(b) depicting the assembly at peak stress ratio. Considering that $E(\theta)$ is such that directions θ and $\theta + \pi$ are physically equivalent, it can always be represented by a Fourier series containing even components. An adequate approximation for the normalized contact orientation distribution can be obtained

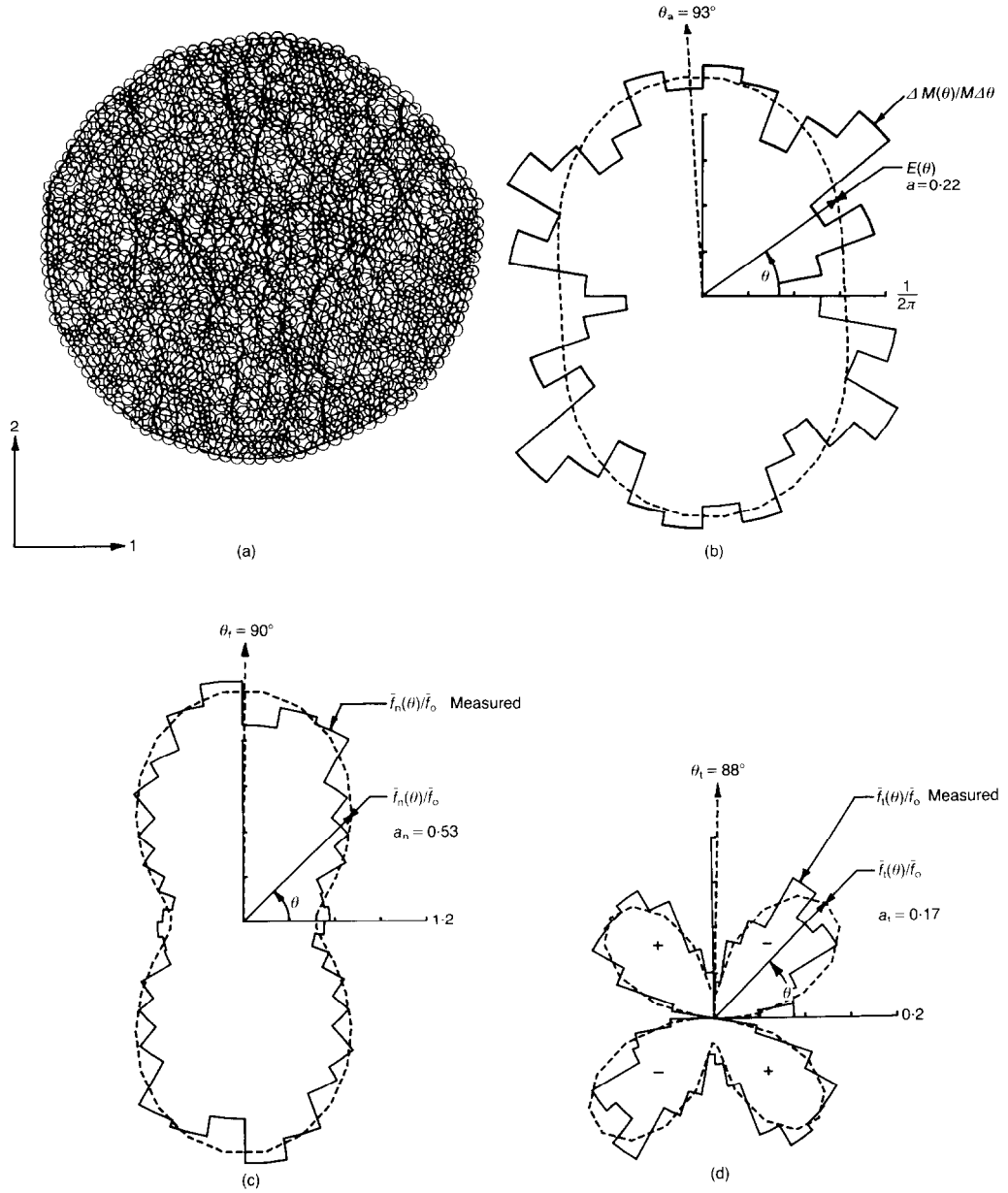

Fig. 4. Distribution of contact normals and average interparticle force components during biaxial compression test: (a) assembly at peak stress ratio; (b) contact normals at peak stress ratio; (c) average normal forces at peak stress ratio; (d) average tangential forces at peak stress ratio

on the basis of a second Fourier component as follows

$$E(\theta) = \frac{1}{2\pi}\{1 + a\cos 2(\theta - \theta_a)\} \qquad (2)$$

where a is a parameter defining the magnitude of anisotropy in contact orientations and θ_a defines the direction of anistropy. When $a = 0$ the distribution is isotropic and $E(\theta) = 1/2\pi$ as illustrated in Fig. 3(b). The predominant trend in the distribution of contact orientations at peak stress ratio can be represented by $E(\theta)$ with $a = 0{\cdot}22$ and $\theta_a \approx \pi/2$ (Fig. 4(b)). It should be noted that the approximation to the observed histogram of contact orientations can be improved by includ-

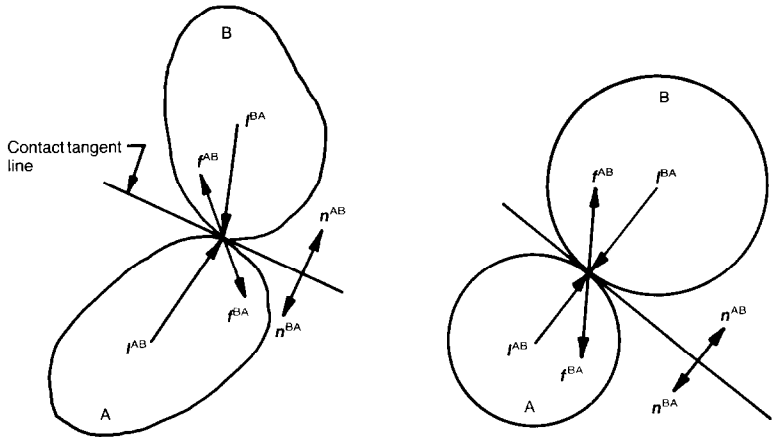

Fig. 5. Contact normals, contact vectors and contact forces

ing higher order Fourier components in equation (2).

The parameter a can be used to trace the evolution of geometrical anisotropy during shear deformations. Physically similar parameters to describe the same process have been used by Biarez & Wiendieck (1963), and Konishi (1978). It can be shown that parameter a is a deviatoric invariant of a symmetric second-order tensor describing the distribution of contact orientations and θ_a is an eigenvector of this tensor. This observation leads to a simple analytical technique to calculate a and θ_a from contact orientation data (e.g. Bathurst, 1985). The description of internal geometry by a so-called fabric tensor appears elsewhere in the literature (e.g. Satake, 1978; Rothenburg, 1980; and Mehrabadi *et al.*, 1982).

For finite assemblies where the spectrum of contact orientations is always discrete, expression (2) is an approximation. Only in the limiting case of an infinite system can $E(\theta)$ be assumed continuous to reflect the notion of geometrical disorder in discrete systems.

In essence, determination of parameters a, θ_a (or a_n, θ_f, a_t and θ_t) can be carried out using relationships such as

$$\int_0^{2\pi} E(\theta) \cos 2\theta \, d\theta = (a/2) \cos 2\theta_a$$

$$\int_0^{2\pi} E(\theta) \sin 2\theta \, d\theta = (a/2) \sin 2\theta_a \qquad (3)$$

Contact vectors

Although the most common geometrical characteristic of a granular assembly is the distribution of particle sizes, it is an inconvenient descriptor of geometry as it relates to load transfer. For example, during the process of deformation, particles having a wide range of sizes may exhibit a preferential affinity to formation or disintegration of contacts with their neighbours and some particles may not participate in load transfer at all.

A characteristic of microscopic geometry that reflects the particle size distribution and is directly related to mechanisms of load transfer is the distribution of distances between each particle centroid and points of contact that transmit force to its immediate neighbours. In this text, vectors connecting centroids of particles and points of contact are referred to as contact vectors (Rothenburg & Selvadurai, 1981). For spherical particles and discs, contact vector lengths are equal to particle radius and orientations of contact vectors are coincident with contact normals. Fig. 5 illustrates the definition for contact vector.

For the general case of particles of arbitrary shape and gradation it is necessary to introduce a joint contact vector length-orientation distribution $S(\boldsymbol{l})$ defining the portion of contacts within a range of contact vectors between $\boldsymbol{l}$ and $\boldsymbol{l} + d\boldsymbol{l}$. The numerical simulations reported in this study showed that contact vector lengths were statistically independent of contact orientations at all stages of sample deformation. Hence, for assemblies of discs (or spheres)

$$S(\boldsymbol{l}) = L(l^c)E(\boldsymbol{n}) \qquad (4)$$

where $\boldsymbol{n}$ is the unit vector used to define the orientation of the contact normal. For plane particles $\boldsymbol{n} = \{\cos(\theta), \sin(\theta)\}$ whereas for spherical particles, components of $\boldsymbol{n}$ will be expressed in terms of spherical angles.

In the subsequent analytical investigation the concept of contact vector emerges naturally from

the analysis of conditions of static equilibrium in assemblies of particles of arbitrary shapes.

CONTACT FORCES

Magnitudes of contact forces in an assembly with irregular geometry vary from contact to contact as depicted in Figs 1, 3(a) and 4(a). Despite the apparent randomness in variation of contact forces, regular trends emerge when normal and tangential components of interparticle forces are averaged over groups of contacts with similar orientations. Normal and tangential contact forces can be referenced to Fig. 5.

The uniform angular distribution of average normal forces illustrated in Fig. 3(c) reflects the fact that the assembly is geometrically isotropic and is under hydrostatic load (initial state). The corresponding tangential components of contact forces averaged over groups of similarly oriented contacts are zero (Fig. 3(d)). Tangential force components can have positive or negative sign to reflect the sense of rotation imparted on the particle. Therefore, zero average tangential force does not imply the absence of tangential forces at contacts.

The angular distribution of average normal forces at the state of peak stress ratio is shown in Fig. 4(c). On average, maximum forces are carried by contacts with orientations close to the direction of maximum principal stress. Minimum average normal forces are associated with contacts oriented along the minimum principal stress direction. The shape of the distribution is similar to the contact orientation distributions considered previously and can be approximated by a similar analytical expression

$$\bar{f}_n(\theta) = \bar{f}_0\{1 + a_n \cos 2(\theta - \theta_f)\} \quad (5)$$

For isotropic assemblies, $\bar{f}_0$ is a constant that represents the average normal force over all contacts in the assembly. For anisotropic assemblies, where the number of contacts in different orientations varies, $\bar{f}_0$ is the measure of average normal contact force when all groups are given equal weight, i.e.

$$\bar{f}_0 = \int_0^{2\pi} \bar{f}_n(\theta)\, d\theta \quad (6)$$

The coefficient a_n defines the magnitude of the directional variation of average normal forces and θ_f defines the direction of maximum average normal force. It should be noted that θ_f and θ_a in (2) are not necessarily coincident with the major principal stress direction. This is, nevertheless, the case for the described biaxial test that does not involve principal stress rotation.

The angular distribution of average tangential forces (Fig. 4(d)) shows four symmetrical peaks for groups of contacts oriented at about 45° to principal stress directions. However, average tangential forces for groups of contacts oriented along principal stress directions remain zero, as at the initial state. Forces on contacts of these two orientations are essentially normal to planes of contact (on average). The alternating sign of average tangential forces is demanded by moment equilibrium for each particle.

A suitable analytical expression to approximate distributions of the type shown in Fig. 4(d) is as follows

$$\bar{f}_t(\theta) = -\bar{f}_0 a_t \sin 2(\theta - \theta_t) \quad (7)$$

where a_t, similar to a_n in (6), defines the magnitude of directional variation of tangential forces and θ_t defines directions in which tangential force is zero on average. The coefficient $\bar{f}_0$ is the average normal force, as defined previously. It is introduced here for convenience as a scaling factor on tangential forces. The negative sign in equation (7) reflects the adopted sign convention when positive tangential forces tend to rotate a particle counter-clockwise.

CHANGES IN ANISOTROPY AND FORCES DURING SHEAR DEFORMATIONS

Detailed microscopic information on a numerically simulated assembly of discs can be used to trace the evolution of microstructure and contact forces during shear deformations. Physical trends in the simulated system become apparent if the complete microscopic information is reduced to a few statistical characteristics such as those introduced in the preceding section.

Evolution of contact orientation distribution

The evolution of contact orientations can be best expressed in terms of parameter a in equation (2) that is essentially proportional to the difference in the number of vertical and horizontal contacts and describes the degree of anisotropy in contact orientations. Fig. 6(a) shows that the degree of anisotropy increases with sample distortion. This trend is due to the overall disintegration of interparticle contacts (Fig. 2(c)). The loss of contacts is most pronounced for contacts oriented along the direction of tensile strain (horizontal strain in this case). Similar trends have been observed in physical tests on photoelastic discs reported by Oda & Konishi (1974a) and from numerical simulation of assemblies of discs reported by Cundall *et al.* (1982) and Thornton & Barnes (1986).

Evolution of average contact forces

In the simulated biaxial test examined here the overall magnitude of contact forces increases. Of primary importance to the subsequent analytical

investigation is the directional variation of average normal forces controlled by the parameter a_n in the expression for the distribution of average normal forces (5). Fig. 6(b) illustrates the evolution of this parameter during the progress of the test. Close inspection of test results shows that the reduction in a_n starts past 2·5% of shear strain whereas the overall macroscopic softening begins later (i.e. 3% shear strain Fig. 2(b)).

Detailed examination of particle movement in this test revealed that the reduction in a_n is related to reorganization of microstructure when the dilation rate is maximum. Dilation is initiated by movement of highly compressed conglomerates of particles that move as rigid blocks and disrupt the assembly. This observation is consistent with physical tests of Drescher & de Josselin de Jong (1972) who identified conglomerates of particles that tend to move as rigid blocks. In general terms, the reduction in a_n reflects the loss of the capacity of rigid blocks to sustain high forces owing to local horizontal spreading of particles that support these blocks.

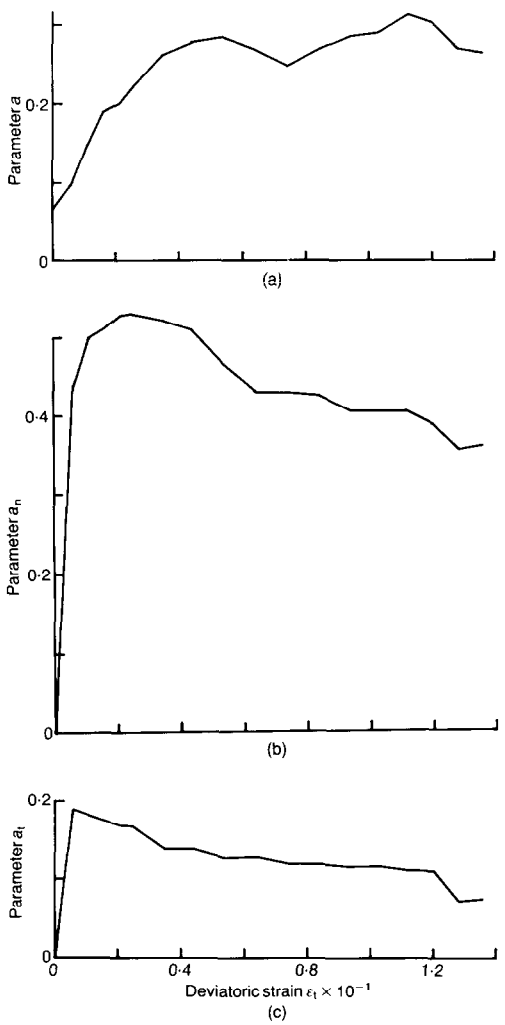

Fig. 6. Evolution of microstructural anisotropy during numerically simulated biaxial compression test: (a) contact anisotropy; (b) normal force anisotropy; (c) tangential force anisotropy

The parameter a_t characterizing the distribution of average tangential components of contact forces features a rapid rise to a peak value (Fig. 6(c)) followed by a slow decline in magnitude. It is apparent from this trend that the assembly is kinematically locked initially and deforms elastically. Nevertheless, even during initial elastic deformations, contacts disintegrate and parameter a increases rapidly. At this stage the tangential forces increase in response to relative translational movement of particles. When the number of contacts where slip is possible reaches some threshold, the assembly becomes kinematically mobile and dilates with further loss of contacts. As contact density decreases, particles have increased rotational freedom and, as a result, tangential forces are slowly released. It should be noted that at all deformation stages in the numerically simulated test the number of contacts where slip occurs was small. The same observation has been reported from similar physical tests on assemblies of photo-elastic discs by Oda & Konishi (1974a).

Relationship between deviatoric load and microstructural parameters

The evolution of microstructural characteristics with shear strain (Fig. 6) bears a qualitative resemblance to familiar stress–strain curves for granular materials. For example, the degree of contact anisotropy (parameter a) varies with shear strain similar to the stress–strain response of a loose granular material. Also, parameter a_n that describes the directional variation of contact forces features the type of softening response usually associated with dense granular materials. This correspondence is not coincidental and it will be shown in the next section that the introduced microscopic parameters are related to the measure of deviatoric load imposed on an assembly of discs as follows

$$\frac{\sigma_{22} - \sigma_{11}}{\sigma_{11} + \sigma_{22}} = \tfrac{1}{2}(a + a_n + a_t) \qquad (8)$$

Fig. 7 presents the stress–strain response in the simulated biaxial compression test expressed in terms of $(\sigma_{22} - \sigma_{11})/(\sigma_{11} + \sigma_{22})$ against shear strain and the quantity $\frac{1}{2}(a + a_n + a_t)$ determined

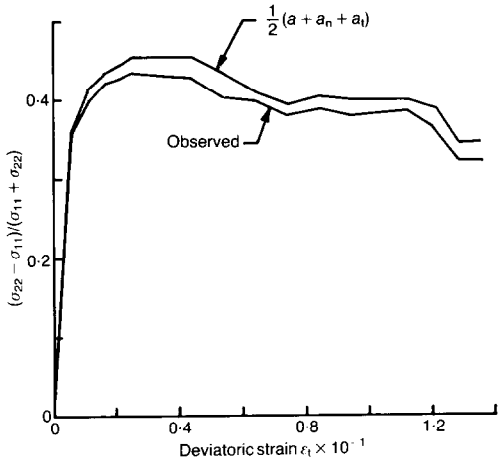

Fig. 7. Assembly stress in terms of coefficients of anisotropy

on the basis of microscopic information. It is visually apparent that relationship (8) accurately relates the macroscopic measure of shear stress with characteristics of microstructure. This expression applies to conditions when the principal direction of stress is coincident with the direction of anisotropy.

STATIC EQUILIBRIUM IN GRANULAR ASSEMBLIES

When discrete point loads are applied at a boundary of a material viewed as a continuum, any statically admissible (generally nonhomogeneous) stress field within the media is such that the volume average of the stress tensor is related to boundary forces as follows (Landau & Lifshitz, 1959)

$$\sigma_{ij} = \frac{1}{V} \sum_{\beta \in S} f_i^{\beta} r_j^{\beta} \quad i, j = 1, 2, 3 \tag{9}$$

where r^{β} are locations of points where loads f^{β} are applied to the sample boundary S. Although equation (9) originates in continuum mechanics, its physical meaning in the context of discrete assemblies can be illustrated by referring to the most common idealized test condition when a rectangular sample of material is confined within frictionless platens (Fig. 8). In this case, equation (9) is simply a statement of force balance between boundary loads specified in terms of stress tensor and boundary forces. To demonstrate this point it is sufficient to calculate the right-hand sum in equation (9) separately for each of the four rectangular platens in Fig. 8. For example, the component σ_{11} (based on equation (9)) can be calculated as follows

$$\sigma_{11} = \frac{1}{V} \sum_{\beta \in S} f_1^{\beta} r_1^{\beta} = \frac{1}{V} \sum_{\beta \in \{ab\}} f_1^{\beta} r_1^{\beta} + \frac{1}{V} \sum_{\beta \in \{bc\}} f_1^{\beta} r_1^{\beta} + \frac{1}{V} \times \sum_{\beta \in \{cd\}} f_1^{\beta} r_1^{\beta} + \frac{1}{V} \sum_{\beta \in \{da\}} f_1^{\beta} r_1^{\beta} \tag{10}$$

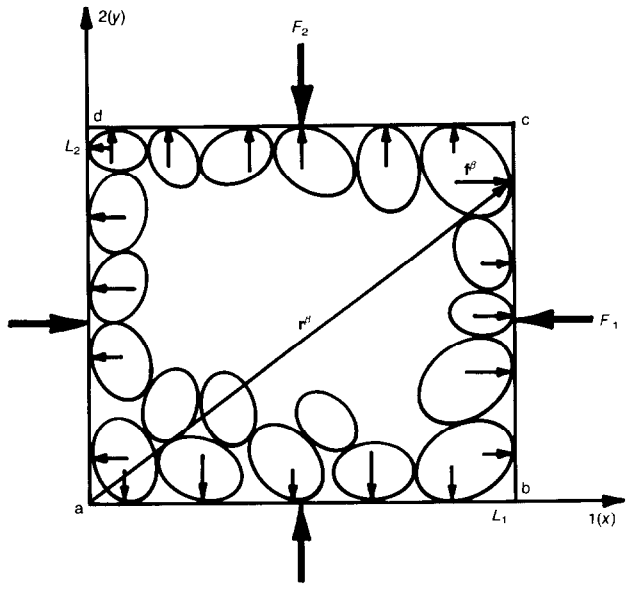

Fig. 8. Idealized granular assembly confined within rectangular platens

Since the platens are considered frictionless, the f_1 component of forces between boundary particles and platens *ab* and *cd* are zero. The remaining sums can be evaluated by noting that all particles adjacent to the platen *bc* have the same *x*-co-ordinates of contact points (i.e. L_1). Similarly, for the platen *da* all *x* co-ordinates are zero. The following chain of calculations complete the illustration

$$\sigma_{11} = \frac{1}{V}\sum_{\beta \in S} f_1^{\beta} r_1^{\beta} = \frac{1}{V}\sum_{\beta \in \{bc\}} f_1^{\beta} r_1^{\beta} + \frac{1}{V}\sum_{\beta \in \{da\}} f_1^{\beta} r_1^{\beta} = \frac{L_1}{L_1 L_2} \times \sum_{\beta \in \{bc\}} f_1^{\beta} = \frac{F_1}{L_2} \tag{11}$$

The same calculations can be done for other components of the stress tensor.

If a sample is confined within an arbitrary shaped boundary and the intent is to study its behaviour under conditions of prescribed macroscopically uniform stress σ_{ij}, boundary contact forces for discrete analysis must be selected as $f_j^{\beta} = \sigma_{ij} n_j^{\beta} A^{\beta}$. Here A^{β} is the area tributary to the particle and $\boldsymbol{n}^{\beta}$ is the orientation of a contact where the load is applied. For any selection of tributary areas, equation (9) gives an exact volume average of stresses over all particles in the volume (if particles are treated as continuum). The difference between the volume average of stresses in particles and the prescribed macroscopic stress diminishes with number of particles in the studied volume.

The relationship (9) is inconvenient from an analytical point of view as it contains positions of boundary particles. A form of this relationship that makes no explicit reference to the shape of the studied volume can be obtained by noting that for any assembly in static equilibrium the following relationship between boundary and internal forces is satisfied (e.g. Rothenburg, 1980)

$$\sum_{\beta \in S} f_i^{\beta} r_j^{\beta} = \sum_{c \in V} f_i^{c} l_j^{c} \tag{12}$$

where $\boldsymbol{l}^{c}$ are contact vectors and $\boldsymbol{f}^{c}$ are contact forces introduced earlier. Comparison of equation (9) and (12) results in the following representation of stress tensor

$$\sigma_{ij} = \frac{1}{V}\sum_{c \in V} f_i^{c} l_j^{c} \quad i, j = 1, 2, 3 \tag{13}$$

This relationship is equally valid for plane and three-dimensional systems. For plane systems, V is the area occupied by the assembly and indices are restricted to $i, j = 1, 2$.

As a function of discrete microscopic parameters, the stress tensor in the form of equation (13) and/or its invariants can be evaluated exactly only when the values of all parameters are precisely known. When this is done using the results of numerical simulations and the stresses are calculated for volumes with progressively larger number of particles it becomes clear that the influence of any single discrete characteristic diminishes with the volume size. Calculations of this nature are illustrated in Fig. 9 showing the ratio $(\sigma_{22} - \sigma_{11})/(\sigma_{11} + \sigma_{22})$ calculated from equation (13) and plotted for subvolumes with progressively increasing number of particles. The trend in the figure suggests that in the hypothetical limit of an infinite system the dependence of volume averages on individual discrete parameters may vanish (the so-called thermodynamic limit in statistical physics, Landau & Lifshitz, 1959). In this limiting case, the discrete spectra of characteristics like contact forces, contact orientations, contact vector length can be assumed to be continuous and described in terms of densities.

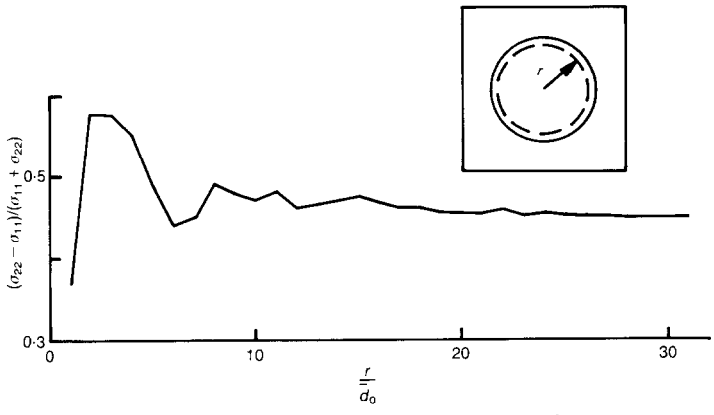

Fig. 9. Influence of assembly size on assembly stress ratio

For plane systems these functions were given by equations (1), (2), (5) and (7).

To represent an infinite sum in equation (13) by an integral expression it is sufficient to note that a group of contacts with contact vectors within an interval l and $l + dl$ with $m_v S(l)\, dl$ terms make the contribution $m_v \bar{f}^c(l)S(l)\, dl$ into the overall volume average. To assess the contribution of all groups it is now sufficient to integrate over all lengths and orientations of contact vectors

$$\sigma_{ij} = m_v \int_V \bar{f}_i^c(l) l_j^c(l) S(l)\, dl \qquad (14)$$

In essence, equation (14) for stress tensor is no more than a statement of static equilibrium in an infinite granular assembly. When an assembly consists of spherical particles or discs and when it is permissible to neglect the statistical dependence between the contact vector lengths and their orientations as well as the dependence of average contact forces on the length of contact vectors, the above relationship can be simplified as

$$\sigma_{ij} = m_v \bar{l}_0 \int_V \bar{f}_i(\boldsymbol{n}) n_j^c(\boldsymbol{n}) E(\boldsymbol{n})\, d\boldsymbol{n} \qquad (15)$$

where $\bar{l}_0$ is the contact vector length averaged over all contacts. For spherical particles and discs with a narrow distribution of radii, the average contact vector length is essentially the average particle radius.

STRESS–FORCE–FABRIC RELATIONSHIP FOR PLANE SYSTEMS

The physical consequence of equation (15) for the stress tensor can be explored by explicitly specifying distributions of contact orientations and average forces. Considering that distributions of average forces were specified previously in terms of normal and tangential components, it is convenient to rewrite the two-dimensional version of equation (15) by introducing $\bar{f}_i(\theta) = \bar{f}_n(\theta) n_i^c + \bar{f}_t(\theta) t_i^c$ where t^c is the unit vector tangent to the line of contact. The expression (15) takes the form

$$\sigma_{ij} = m_v \bar{l}_0 \int_0^{2\pi} [\bar{f}_n(\theta) n_i^c n_j^c + \bar{f}_t(\theta) t_i^c n_j^c] E(\theta)\, d\theta \qquad i, j = 1, 2 \quad (16)$$

It should be noted that expression (16) does not necessarily assure the symmetry of the stress tensor for aribtrary $\bar{f}_t(\theta)$ and $E(\theta)$. The condition of symmetry can be written as

$$\sigma_{ij} - \sigma_{ji} = m_v \bar{l}_0 \int_0^{2\pi} \bar{f}_t E(\theta)\, d\theta = 0 \qquad (17)$$

From a physical point of view the above relationship reflects the condition of moment equilibrium because the sum of tangential forces acting on each particle must be zero (if forces are considered to be transferred through point contacts). The symmetry condition (17) must be looked on as a constraint on the distributions involved in this expression. For conditions when the direction of contact anisotropy θ_a is coincident with the principal directions of force, expressions for $\bar{f}_t(\theta)$ and $E(\theta)$ in the form (7) and (2) satisfy this constraint. More general conditions of non-coincidence of the direction of anisotropy and the principal direction of stress have been explored by Rothenburg (1980).

If distributions (2), (5) and (7) with $\theta_a = \theta_f = \theta_t$ are substituted into equation (16) and integration is performed, the following expressions for stress tensor components can be recovered

$$\sigma_{11} = \frac{m_v \bar{l}_0 \bar{f}_0}{2} \left\{1 + \frac{a a_n}{2} + \frac{1}{2}(a + a_n + a_t) \cos(2\theta_a)\right\}$$

$$\sigma_{22} = \frac{m_v \bar{l}_0 \bar{f}_0}{2} \left\{1 + \frac{a a_n}{2} - \frac{1}{2}(a + a_n + a_t) \cos(2\theta_a)\right\}$$

$$\sigma_{12} = \sigma_{21} = \frac{m_v \bar{l}_0 \bar{f}_0}{2} \left\{\frac{1}{2}(a + a_n + a_t) \sin(2\theta_a)\right\} \qquad (18)$$

The above expressions for components of the stress tensor immediately suggest that the major principal direction of stress is θ_a (i.e. the direction of anisotropy in contact orientations as well as the assumed preferred direction for average forces). The invariants of the stress tensor (in the form of parameters of the Mohr circle) are as follows

$$\sigma_n = \frac{\sigma_{11} + \sigma_{22}}{2} = \frac{m_v \bar{l}_0 \bar{f}_0}{2} \left(1 + \frac{a a_n}{2}\right) \qquad (19)$$

$$\sigma_t = \sqrt{\left[\left(\frac{\sigma_{11} - \sigma_{22}}{2}\right)^2 + \sigma_{12}^2\right]} = \frac{m_v \bar{l}_0 \bar{f}_0}{4}(a + a_n + a_t) \qquad (20)$$

The ratio of the above two invariants is independent of the number of contacts and is as follows

$$\frac{\sigma_t}{\sigma_n} = \frac{\frac{1}{2}(a + a_n + a_t)}{(1 + (a_n a/2))} \qquad (21)$$

The latter quantity is frequently associated with the mobilized angle of friction for cohesionless material (i.e. $\sin \phi = \sigma_t/\sigma_n$). However, the derived relationships are for any plane granular assembly of discs, irrespective of specific types of particle interactions. This relationship relates characteristics of microstructural response with the level of deviatoric load. For brevity, expression (21) can

be referred to as the stress–force–fabric relationship.

For the simulated cohesionless assemblies, parameters a, a_n, a_t are such that the product $aa_n/2$ in the denominator of equation (21) is small and can be neglected, resulting in the conceptually simple relationship $\sigma_v/\sigma_n = \frac{1}{2}(a + a_n + a_t)$. This simplified expression suggests that the capacity of a cohesionless granular assembly to carry deviatoric loads is due to its ability to develop anisotropy in contact orientations or to withstand directional variation of average contact forces. All contributions to deviatoric load capacity are additive. The verification of this relationship was presented and is illustrated in Fig. 7. If the term $aa_n/2$ in equation (21) is not neglected, the theoretical and experimental curves in Fig. 7 become practically indistinguishable. This is hardly surprising as equation (21) is no more than a condition of static equilibrium in an infinite assembly. It appears that a 1000 particle assembly adequately models an infinite system for purposes of force balance. It should be noted that the relationship (21) has been verifed by numerically simulating tests with different stress paths that involve no stress rotation (Bathurst, 1985). These simulations resulted in the same level of accuracy as the biaxial compression test that is used here as an illustration.

DISCUSSION OF FINDINGS

Theoretical developments presented in this Paper are based on detailed investigation of conditions of static equilibrium in granular assemblies where particles are assumed to interact by means of contact forces. Under deviatoric loads the magnitudes of forces carried by contacts are strongly biased by the orientation of contacts. Contacts oriented along the direction of major principal stress carry higher forces whereas lower forces are associated with contacts oriented in the minor principal stress direction. However, the force per contact for contacts of any given orientation depends on the number of contacts with this orientation. This delicate balance between internal forces and external loads is expressed in the derived relationship for stress tensor in terms of average forces and the distribution of contact orientations.

To make the mathematics of discrete systems manageable it was necessary to use a standard technique of classical statistical physics where studies of large but finite systems are replaced by the analysis of infinite systems. It was shown that the force balance relationships derived for an infinite system provide an accurate description for assemblies comprising as little as 1000 particles. For such systems, the stress tensor is an average characteristic of forces acting on about 2000 physical contacts. However, macroscopic deformational properties of the same size assembly may be controlled by a relatively small number of particle clusters.

From a physical point of view the most significant result of this investigation is the introduction of parameters that quantify essential features of microstructure such as anisotropy in contact orientations and average contact forces. These parameters were shown to be directly related to the mobilized angle of friction which is the most common measure of shearing resistance (i.e. sin $\phi = \frac{1}{2}(a + a_n + a_t)$).

There have been several other attempts to repartition the stress tensor for granular assemblies into components associated with distinctly different micromechanical aspects of load transmission (e.g. Cundall & Strack, 1983; Mehrabadi *et al.* 1982, and Thornton & Barnes 1986). In all cases an attempt is made to identify contributions of normal and tangential components of contact forces as well as fabric anisotropy to a measure of deviatoric load. Expression (21) appears to be a uniquely simple relationship that is directly verifiable and conveys a clear statement of the additive contributions of different mechanisms of load transmission to the shear capacity of granular materials.

Of the three strength components that contribute to the overall shearing resistance, the least significant is the one that is associated with tangential forces. For example, at the limiting state of the simulated test the parameter a_t accounts for only 11% of sin ϕ at large strains. To some extent the decomposition of shearing resistance into components related to anisotropy and directional variation of contact forces obscures the role of interparticle friction. Detailed observations reported by Bathurst (1985) suggest that only a small interparticle friction is necessary to provide stability to clusters of particles that carry high normal forces. It appears that these highly oriented clusters of particles are responsible for the component of strength associated with the parameter a_n which is the largest contributor to the overall shearing resistance (55% of sin ϕ at large strains). The large values of a_n determined from the simulated test point out that granular assemblies tend to transfer load along preferential paths characterized by high normal forces. These load paths are clearly identifiable in both numerical simulations by the Authors and others (e.g. Cundall & Strack, 1979; Thornton & Barnes 1986) and in physical tests on assemblies of photo-elastic discs (e.g. de Josselin de Jong & Verruijt 1969, Oda & Konishi, 1974a). When the assembly dilates, the clusters of particles that transfer high normal forces lose their

lateral support and can no longer sustain high contact forces. Macroscopically this phenomenon is manifested as strain softening.

Although anisotropy in contact orientations, expressed in terms of parameter a, appears as a positive contributor to the overall shearing resistance (about 40% in the limiting state), development of anisotropy is a manifestation of damage owing to preferential loss of interparticle contacts. Although a is a positive contribution to strength, the damage caused by loss of contacts ultimately reduces a_n. In view of the decomposition of shear strength according to equation (8), parameters a, a_n and a_t can be looked on as additive strength components that characterize the state of microstructure.

REFERENCES

Bathurst, R. J. (1985). *A study of stress and anisotropy in idealized granular assemblies.* PhD dissertation, Queen's University at Kingston, Canada.

Bathurst, R. J. & Rothenburg, L. (1988a). Micromechanical aspects of isotropic granular assemblies with linear contact interactions. *J. Appl. Mech. Am. Soc. Mech. Engrs* **55,** 17–23.

Bathurst, R. J. & Rothenburg, L. (1988b). Note on a random isotropic granular material with negative Poisson's ratio. *Int. J. Engng Sci.* **26,** No. 4, 373–383.

Biarez, J. & Wiendieck, K. (1963). La comparaison qualitative entre l'anisotropie mécanique et l'anisotropie de structure des milieux pulvérulents. *C. R. Hebd. Séanc. Acad. Sci., Paris* **256,** 1217–1220.

Cundall, P. A. & Strack, O. D. L. (1979a). A discrete numerical model for granular assemblies. *Géotechnique*, **29,** No. 1, 47–65.

Cundall, P. A. & Strack, O. D. L. (1979b). The development of constitutive laws for soil using the distinct element method. *Third int. conf. numerical methods in geomechanics, Aachen*, 289–298.

Cundall, P. A., Drescher, A. & Strack, O. D L. (1982). Numerical experiments on granular assemblies; measurements and observations. *IUTAM conf. Deformation and failure of granular materials, Delft*, 355–370.

Cundall, P. A. & Strack, O. D. L. (1983). Modelling of microscopic mechanisms in granular material. *Proc. US-Jap. seminar on new models and constitutive relations in the mechanics of granular materials*, Jenkins, J. T. & Satake, M. (eds).

Dantu, P. (1957). Contribution à l'étude mécanique et géométrique des milieux pulvérulents. *Proc. 4th Int. Conf. Soil Mech.* **1,** 144–148.

Dantu, P. (1968). Étude statistique des forces intergranulaires dans un milieu pulvérulent. *Géotechnique* **18,** No. 1, 50–55.

de Josselin de Jong, G. & Verruijt, A. (1969). Étude photo-élastique d'un empilement de disques. *Can. Grpe. Fr. Etude Rheol.*, No. 2, 73–86.

Drescher, A. & de Josselin de Jong, G. (1972). Photoelastic verification of a mechanical model for the flow of a granular material. *J. Mech. Phys. Solids* **20,** 337–351.

Horne, M. R. (1965). The behaviour of an assembly of rotund, rigid, cohesionless particles I & II. *Proc. R. Soc.* **286,** 62–97.

Konishi, J. (1978). Microscopic model studies on the mechanical behaviour of granular materials. *Proc. US.-Jap. seminar on continuum-mechanical and statical approaches in the mechanics of granular materials, Tokyo*, Jenkins, J. T. & Satake, M. (eds), 27–45.

Landau, L. D. & Lifshitz, E. M. (1959). *Statistical physics: course of theoretical physics* **5.** Oxford: Pergamon Press, 1–2.

Mehrabadi, M. M., Nemat-Nasser, S. & Oda, M. (1982). On statistical description of stress and fabric in granular materials. *Int. J. Num. Anal. Meth. Geomech.* **6,** 95–108.

Oda, M. (1972a). Initial fabrics and their relations to mechanical properties of granular materials. *Jap. Soc. Soil Mech. Fdn Engng* **12,** No. 1, 17–36.

Oda, M. (1972b). The mechanism of fabric changes during compressional deformation of sand. *Jap. Soc. Soil Mech. Fdn Engng* **12,** No. 2, 1–18.

Oda, M. (1972c). Deformation mechanism of sand in triaxial compression tests. *Jap. Soc. Soil Mech. Fdn Engng* **12,** No. , 45–63.

Oda, M. & Konishi, J. (1974a). Microscopic deformation mechanism of granular material in simple shear. *Jap. Soc. Soil Mech. Fdn Engng* **14,** No. 4, 25–38.

Oda, M. & Konishi, J. (1974b). Rotation of principal stresses in granular material in simple shear. *Jap. Soc. Soil Mech. Fdn Engng* **14,** No. 4, 39–53.

Rothenburg, L. (1980). *Micromechanics of idealized granular systems*, PhD dissertation, Carleton University, Ottawa.

Rothenburg, L. & Selvadurai, A. P. S. (1981). A micromechanical definition of the cauchy stress tensor for particulate media. *Proc. Int. Symp. on Mech. Behaviour of Structured Media.* Selvadurai, A. P. S., (ed.), Ottawa.

Satake, M. (1978). Constitution of mechanics of granular materials through the graph theory. *Proc. US.-Jap. seminar on Continuum-mechanical and statistical approaches in the mechanics of granular materials, Tokyo*, Jenkins, J. T. & Satake, M. (eds), 47–62.

Schneebeli, G. (1956). *C. R. Hebd. Séanc. Acad. Sci., Paris* **243,** 125.

Thornton, C. & Barnes, D. J. (1986). Computer simulated deformation of compact granular assemblies. *Acta Mechanica*, **64,** 45–61.